Modeling and Experimental Analysis of Interlaced Hot Glycol Defrost System

Harun DENIZLI[1]*, Mustafa ZABUN[1], Burhan YORUK[1]

[1]Friterm Thermal Devices Inc.,
Tuzla, Istanbul, Türkiye
harundenizli@friterm.com
mustafazabun@friterm.com
burhanyoruk@friterm.com

ABSTRACT

There are several methods available for defrosting or deicing the surfaces of heat exchangers in cold rooms. One of these methods is interlaced glycol (brine) defrost system, where hot liquid is circulated through a separate circuit within the evaporator to facilitate the defrosting process. In this study, a mathematical model has been developed to analyze interlaced brine defrost. Experimental results show that developed model is predicting key defrost parameters very well. Besides, based on the existing literature, the performance and duration of interlaced glycol defrost are aimed to be predicted. This method, which consists of one main loop and two sub-routines, determines the exit temperature of glycol through an iterative approach. Ultimately, the glycol mass flow rate is determined, allowing glycol to enter the tray at the desired temperature and exit the coil at the required temperature. To validate the developed methodology, a prototype is manufactured and placed in a test chamber. Numerous tests had been conducted under various conditions to verify the methodology's accuracy. To validate this methodology, tests were conducted at four different Reynolds numbers. These Reynolds numbers were selected to represent three different flow regimes (laminar, transition, and turbulent). Based on the results of these experiments, methodology's performance under different flow regimes has been observed. As a result of the comparisons made, it has been observed that the experimental data is consistent with the mathematical model

1. INTRODUCTION

Heat exchangers are integral to numerous industrial processes, ranging from power generation to chemical manufacturing. These devices facilitate the efficient transfer of heat between two fluids, ensuring optimal temperature control and energy efficiency. In the realm of HVAC (Heating, Ventilation, and Air Conditioning) systems, heat exchangers are essential for maintaining comfortable indoor climates. Additionally, in the automotive industry, they play a critical role in engine cooling and maintaining cabin comfort conditions. With the advancements in technology, heat exchangers continue to evolve, offering improved efficiency and sustainability across a diverse range of applications. Growing industrial demands and environmental targets have heightened the significance of heat exchanger performance(Patel, 2023).

Experimental and numerical studies have been conducted to improve the performance of heat exchangers. Al-Obaidi et al. worked to optimize the performance of a heat exchanger involved in a VCC cycle. They achieved the highest COP and pressure ratios at a specific water flow rate.(Al-Obaidi et al., 2020)

One of the major energy losses of the coolers, which is one of the most important heat exchangers, is the defrosting process. During this process, a certain heat load is introduced into the room, so we need to melt maximum frost with minimum energy. Various methods are being used for this purpose. The most popular methods include electric heater defrost, hot gas defrost, and glycol defrost. Citarella et al. introduces a novel approach for determining the optimal initiation time for defrosting in a medium temperature refrigeration system utilizing the hot-gas bypass defrosting method(Citarella et al., 2022). Hoffenbecker et al. outlines the creation, verification, and utilization of a dynamic model to forecast the heat and mass transfer consequences linked with an industrial air-cooling evaporator throughout a hot gas defrosting sequence.(Hoffenbecker et al., 2005)

Some studies have been conducted in the literature on interlaced glycol defrost in heat exchangers. The experiments of Haglund Stignor et al. conducted with two different cooling coils led to the conclusion that the Gnielinski correlation provides good agreement for predicting heat transfer performance on the liquid side of a cooling coil cooled by a liquid secondary refrigerant, within a range of $50 < Re < 1700$, assuming a new entrance length is formed after each U-bend.(Haglund Stignor et al., 2007). Patrick Finn et al. prepared a model using finite element analysis. The model

was verified using experimental data from a set of tests conducted for both electric and hot gas defrost modes. Optimal defrost efficiencies were attained with the least defrost powers, despite the necessity for a considerably longer defrost duration.(Finn et al., 2012)

In this study, inspired by the findings from existing studies, a mathematical model will be developed for the interlaced glycol defrost method based on the Gnielinski correlation. The model to be developed is valid for conditions where there is no forced convection on the air side and there is no special equipment (Suction Hood i.e. (Denizli & Zabun, n.d.)) that will contribute to the defrost process. This mathematical model will involve an iterative solution process, and experimental studies will be conducted for validation. The experimental results will be compared with the theoretical results obtained from the model. This comparison will be carried out across three different flow regimes (laminar, transition, and turbulence).

2. MATHEMATICAL MODEL

2.1 Overview

Defrost calculations consist of 1 main loop and 2 subroutines. In the first subroutine, the mass flow rate providing the inlet and outlet temperatures of glycol on the coil side is calculated. In the second subroutine, while the inlet temperature and mass flow rate are known in the tray, the outlet temperature is calculated. In the main loop, using these two subroutines, the tray outlet temperature is taken as the coil inlet temperature, and the calculated mass flow rate converges to the previous cycle. As a result, the mass flow rate that allows glycol to enter the tray at the given temperature and exit from the coil at the desired temperature is determined. Based on this mass flow rate, other calculations are performed.

3.2 Thermal Model of the Coil Side

The following domain is considered on the coil side;

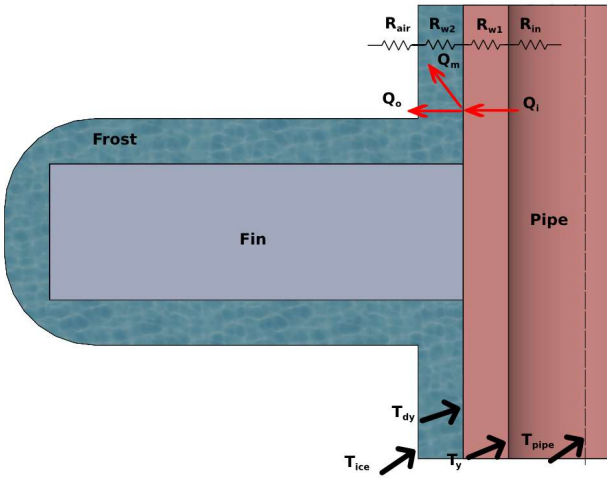

Figure 1: Thermal model of coil side

An efficiency algorithm has been created using the heat balance on the outer surface of the pipe in calculations. The defrost time has been calculated based on this efficiency. It is assumed that a part of the heat coming from the glycol at the average temperature of T_{sm} to the outer surface of the pipe at the temperature T_{dy} is transferred to the environment, and the remainder is used for defrosting. Efficiency is defined as the ratio of the heat used for defrosting to the total transferred heat.

When writing the heat balance, resistances have been taken as follows;

R_{in}: convection thermal resistance of the glycol side based on Gnielinski correlation,
R_{w1}: conduction thermal resistance of the pipe
R_{w2}: conduction thermal resistance of the frost

R_{air}: free convection thermal resistance of the airside

$$R_{w1} = \frac{\ln \frac{Ddf_{out}}{Ddf_i}}{2\pi L_{total} k_{tube}} \quad (1)$$

$$R_{w2} = \frac{\ln \frac{Ddf_o}{Ddf_{out}}}{2\pi L_{total} k_{frost}} \quad (2)$$

Another assumption made in the calculations is the inclusion of the R_{w2} resistance in the R_{air} side. With this assumption, the calculation algorithm has been simplified with an error of less than 3%. The calculation of fin efficiency is obtained from the VDI Heat Atlas book.

$$\alpha_{fr} = \frac{1}{\frac{1}{h_p} + \frac{\delta_f}{k_f}} \quad (3)$$

$$R_{air} = \frac{1}{\alpha_{fr}.(\eta_f A_f + A_p)} \quad (4)$$

3.3 Calculation Steps

Defrost calculations consist of the following steps;

3.3.1 *Determination of material properties:* All physical properties (density, thermal conductivity, etc.) to be used in calculations are determined using Coolprop subfunctions.

3.3.2 *Performing geometric calculations:* Areas, lengths, and masses are calculated based on the circuit/pass number and given geometry.

3.3.3. *Performing preliminary thermal and flow calculations:* Correlations to be used in calculations such as fin efficiency, fluid-side heat transfer coefficient, pressure drop is written.

3.3.4. *Determination of thermal resistances and overall heat transfer coefficients*: Resistances that defined in the coil thermal model section are calculated.

3.3.5. Determination of the amount of frost to be melted and the approximate glycol flow rate: The amount of frost to be melted is determined based on the given frost thickness. As an initial guess, the mass flow rate of ethylene glycol is estimated for the specified temperatures.

3.3.6. Subroutine for calculating the mass flow rate to provide inlet and outlet temperatures of glycol: A subroutine is created to calculate the mass flow rate of glycol using the assumptions described in the thermal model section and the ε-NTU method. The loop calculations are based on the convergence of the amount of heat transferred according to the average glycol temperature.

3.3.7. *Determination of tray geometric calculations and thermal resistances:* Area and thermal resistances are calculated based on the number of pipes/circuits in the tray.

3.3.8. *Step-by-step subroutine to calculate the coil outlet temperature:* The coil is divided into control volumes. Total heat transfer from tray and the tray outlet temperature is calculated using the determined mass flow rate of glycol.

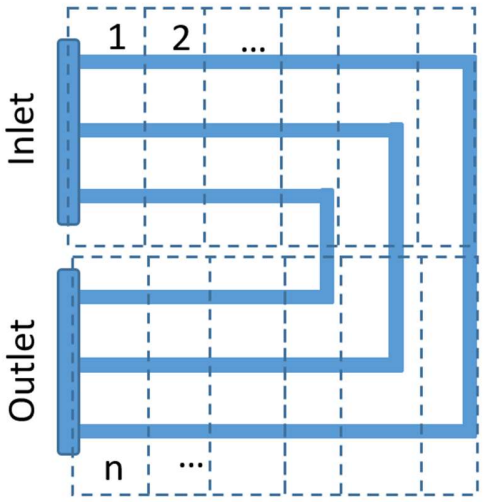

Figure 2: Calculation domain of tray side.

At this domain, free convection heat transfer from the bottom and top of the tray to the surroundings is considered. Insulation on the tray is included in the thermal resistances. The heat loss from glycol is taken as the enthalpy difference for the next control volume, and the control volume temperature of glycol is calculated from the obtained enthalpy.

3.3.9. *Main loop:* The tray outlet temperature is taken as the coil inlet temperature using the coil and tray subroutines. By using the subroutine, mentioned in 3.3.6, new mass flow rate is calculated. Then based on this mass flow rate, new outlet temperature of tray is calculated. This iterative approach is ensuring convergence of the calculated mass flow rate to the previous step.

3.3.10. *Main calculations:* Parameters such as defrosting time, collector diameters, etc. are calculated using the determined mass flow rate. Defrosting involves preheating, phase change, and drying stages. The defrost time can be directly calculated using the coil subprogram. In addition, the coil mass also needs to be heated up to the final drying temperature from approximate evaporation temperature.

Finally, the required energy (E_{df_total}), defrost efficiency, and defrost power are used to calculate the defrost time.

3. EXPERIMENTAL SETUP

The current experiments are designed to examine the defrost time and ethylene glycol outlet temperature. The geometric properties of the tested unit are given in the table below.

Table 1: Geometric properties of tested unit

Parameter	Unit	Value
Geometry	-	M3535
Pipe Diameter	mm	12
Pipe Thickness	mm	0,32
Number of Tube	-	16
Number of Row	-	6
Finned Length	mm	1300
Material of Fin	-	Aluminum
Fin Thickness	mm	0,2

Therefore, there are two different experimental setups here. The first setup is the cooling room arrangement, where frosting on the product will be induced by supplying moist air to the evaporator. Then, in the second setup, which is the ethylene glycol defrost system with electric heaters, heated ethylene glycol containing electric heaters will be sent to the system as a secondary fluid for defrosting.

3.1 Test Conditions

Tests were carried out under 4 different conditions. These conditions are given in Table 2.

Table 2: Test Conditions

Parameter	Unit	Test 1	Test 2	Test 3	Test 4
Inlet Ethylene Glycol Temperature	[°C]	30	30	30	30
Outlet Ethylene Glycol Temperature	[°C]	4,72	20,33	23,5	24,59
Ethylene Glycol Flow	[m3/h]	0,124	0,75	0,124	1,5
Reynolds Number	-	250	1800	3300	4270
Amount of Melted Water	[kg]	10,45	10,46	10,45	10,42
Air Side Pressure Drop	[Pa]	72	72	72	72
Room Temperature	[°C]	0	0	0	0
Evaporation Temperature	[°C]	-8	-8	-8	-8

3.2 Cooling Room

The cold room will be conducted in the calorimetric chamber (Figure 3).

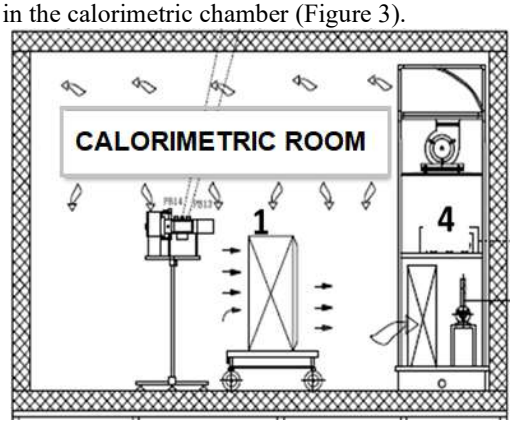

Figure 3: Conceptual visualise of calorimetric room

The calorimetric room is an insulated room where the temperature is controlled by precise heaters. Moisture is supplied to the room as warm vapor, inducing frost formation on the product.

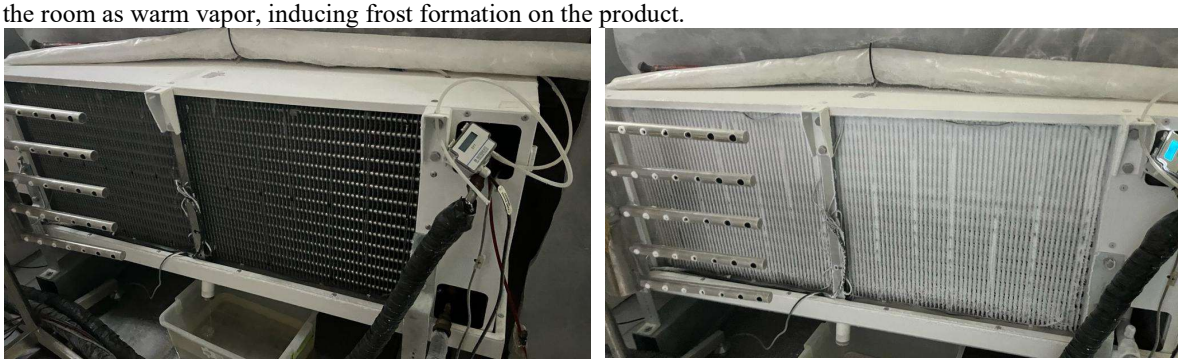

Figure 4: Frosted and unfrosted version of the unit

During the testing, it is necessary to maintain a constant amount of frost because the aim was to carry out the tests under the same conditions. Therefore, a parameter needs to be established to determine the frost amount. This parameter was selected as the air-side pressure drop. When the air-side pressure drop reached a certain level, we initiated the defrost process by stopping the cooling side. The amount of melted water was also measured to verify the

frost amount. Consequently, the frost amount was stabilized. In the mathematical model, frost thickness is assumed to be evenly distributed across all heat transfer surfaces. Therefore, the amount of frost is taken from this data and entered into the mathematical model as input. Thermophysical properties of frost has been evaluated by with ASHRAE correlations.

3.3 Glycol (Brine) Defrost System

Glycol defrost is a secondary system that involves a separate circuit within the heat exchanger to melt the frost formed on the fin and tube surfaces. This method offers advantages such as energy efficiency, controlled heating and reduced thermal load on the room. However, it also has disadvantages, including higher initial costs, maintenance requirements, and space needs. In contrast, defrosting with electric heaters provides lower initial costs and ease of maintenance but has drawbacks in terms of energy efficiency and equipment lifespan. The choice of method depends on specific application requirements and economic considerations. The glycol defrost system operates as a secondary system. This system comprises a glycol tank with precision electric heaters. Heated glycol is then sent to the coil through a pump. The cooled glycol returns to the tank and is reheated. The glycol flow rate is measured using a magnetic flow meter located on the main line. The accuracy of the turbine flow meter is 2%, the accuracy of the air side differential pressure sensor is ± 5 Pa and the accuracy of the temperature sensors is ± 0.5 °C.

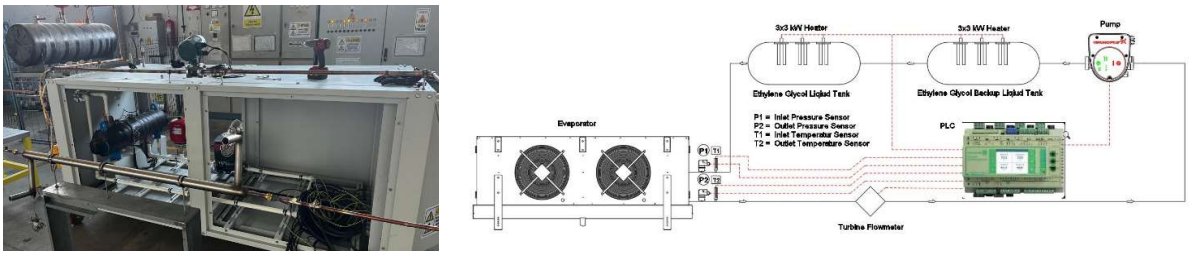

Figure 5: General view of glycol-defrost system

4. RESULTS

The tests were conducted for four different glycol flow Reynolds numbers. The aim here is to observe the performance of the mathematical model in three different flow regimes: laminar, transitional, and turbulent. A multistage pump was used in this test setup, and the tests were conducted based on the different flow rates provided by the pump. The Reynolds numbers of glycol at these flow rates are 250, 1800, 3300, and 4270.

Temperature graphs taken from the fin surface and ethylene glycol outlet temperature for four different Reynolds numbers are presented in Figure 6.

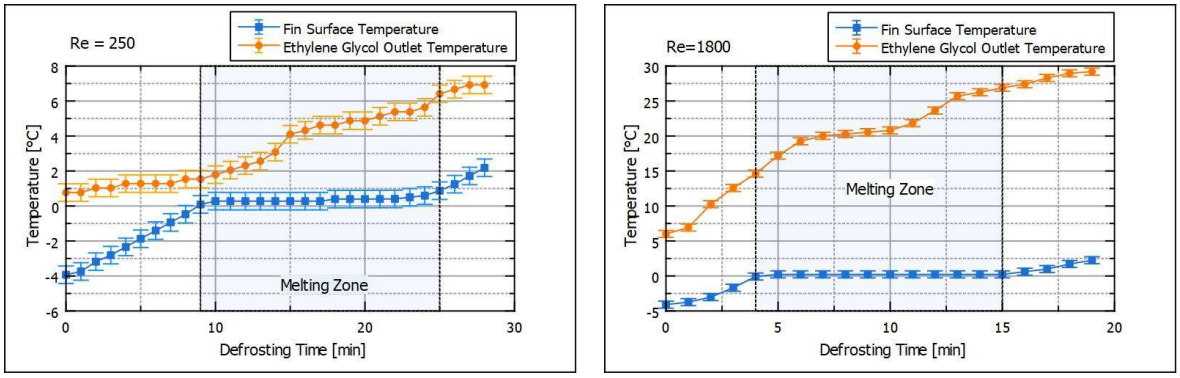

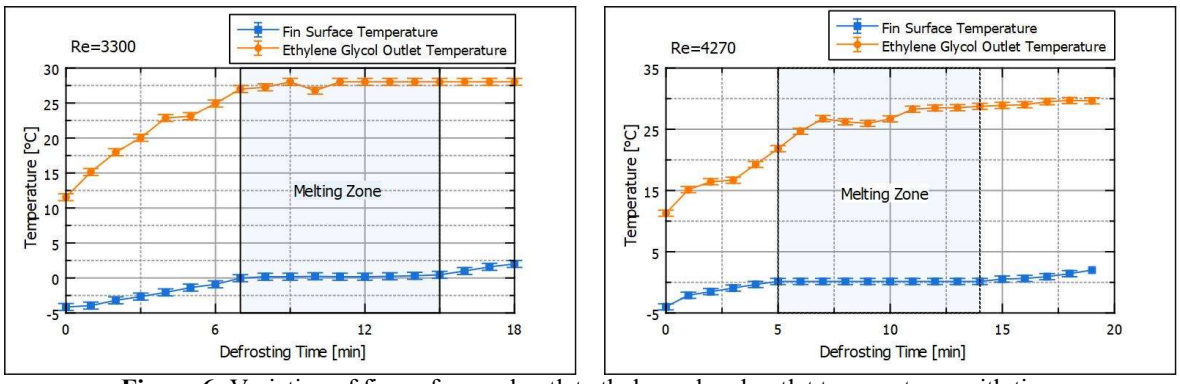

Figure 6: Variation of fin surface and outlet ethylene glycol outlet temperatures with time

The tracking of the start and end of the tests was provided with temperature sensors attached to the product fin surfaces. When the average of surface temperatures taken from five different points exceeds 2°C, the defrost process is considered to be completed. The durations taken for all tests and the determination of the time when defrosting was completed are graphically presented in Figure 7.

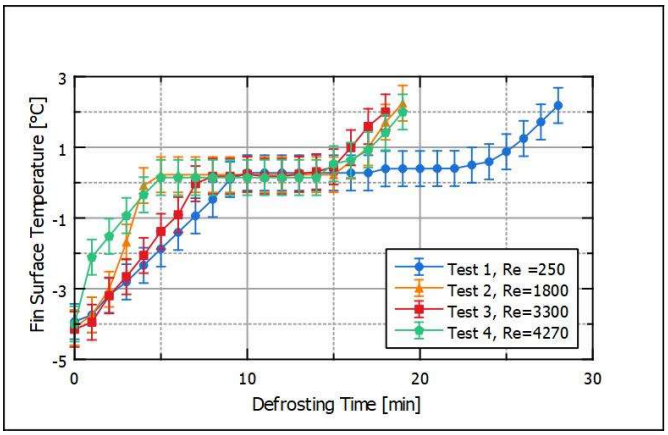

Figure 7: Variation of fin surface and ethylene glycol outlet temperatures with time

The comparison of the two outputs of the mathematical model, namely the glycol outlet temperature and the melting time, with the tests is presented in Figure 8. The curves shown in blue represent the curves drawn by the mathematical model, while the points indicate the test results.

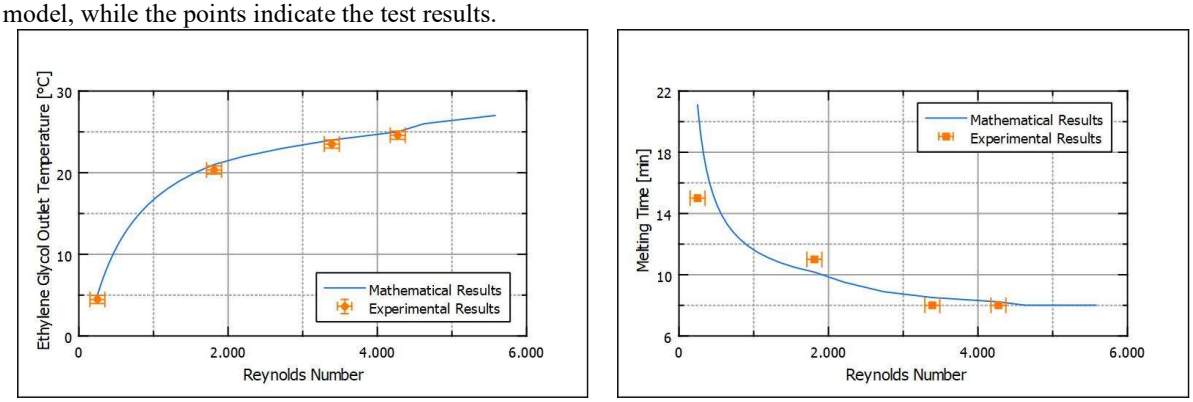

Figure 8: Comparison of experimental glycol outlet temperature and melting time with the mathematical model.

5. CONCLUSIONS

The aim of this study is to develop a mathematical model for predicting the performance of glycol defrost systems designed to prevent icing in heat exchangers during the design phase. Since this model directly affects design, production, and cost parameters, it is an important parameter for heat exchanger manufacturers. In line with this objective, after reviewing the studies in the literature, it is observed that the test results are consistent with the developed mathematical model results.

Table 3: Errors on glycol outlet temperature and melting time

Reynolds Number	Glycol Outlet Temperature Error (%)	Melting Time Error (%)
250	%5,60	%28,84
1800	%3,18	%8,27
3300	%1,75	%6,32
4270	%1,66	%3,50

As observed in Table 3, generally, an error rate of less than 10% is noted. However, a significantly higher error rate is observed only for Reynolds 250, primarily due to the mathematical model defining excessively long melting times at very low Reynolds numbers. Hence, the utilization of this model is deemed inappropriate at very low Reynolds numbers, which are typically not encountered in industrial applications.

When examining the behavior of the mathematical model and tests in Figure 8, it is evident that as the Reynolds number increases, the rate of increase in glycol outlet temperature and the rate of decrease in melting time diminish. Approximately, when the Reynolds number exceeds 4500, the changes in outlet temperature and melting time become negligibly small. As a conclusion, parameters that are calculated with this developed mathematical model can be effectively used to design defrost systems for heat exchangers.

As future work, we aim to test and further develop this mathematical model by considering different frost masses and varying ethylene glycol ratios.

NOMENCLATURE

The nomenclature should be located at the end of the text using the following format:

A	area	(m2)
df	diameter	(m)
h	heat transfer coefficient	($W/(m^2K)$)
L	length	(m)
η	efficiency	(-)

Subscript

f	total fin
p	bare tube
i	inner of tube
o	outer of frost and tube
out	outer of tube
fr	frost

REFERENCES

Al-Obaidi, A. S. M., Naif, A., & Al-Harthi, T. K. (2020). Optimization of the Performance of Vapour Compression Cycle using Liquid Suction Line Heat Exchanger. *Journal of Thermal Engineering*, *6*(2), 201–210. https://doi.org/10.18186/THERMAL.730765

Citarella, B., Viscito, L., Mochizuki, K., & Mauro, A. W. (2022). Defrosting frequency optimization in a cooling system: Minimization of energy consumption vs reduction of the number of on/off cycles per hour. Definition of a methodology and assessment of commercial methods based on experiments. *Applied Thermal Engineering*, *213*(April), 118796. https://doi.org/10.1016/j.applthermaleng.2022.118796

Denizli, H., & Zabun, M. (n.d.). *ODA SOĞUTUCULARDA DEFROST FLAP'İN DEFROST ESNASINDA ODAYA*

OLAN ISI KAZANCINA ETKİSİNİN NÜMERİK OLARAK İNCELENMESİ.

Finn, D. P., Cabello-Portoles, A., Smyth, S., & Brophy, B. (2012). *Evaluation Of Defrost Options For Secondary Coolants In Multi-temperature Indirect Transport Refrigeration: Mathematical Modelling & Sensitivity Analysis*.

Haglund Stignor, C., Sundén, B., & Fahlén, P. (2007). Liquid side heat transfer and pressure drop in finned-tube cooling-coils operated with secondary refrigerants. *International Journal of Refrigeration*, *30*(7), 1278–1289. https://doi.org/10.1016/j.ijrefrig.2007.02.007

Hoffenbecker, N., Klein, S. A., & Reindl, D. T. (2005). Hot gas defrost model development and validation. *International Journal of Refrigeration*, *28*(4), 605–615. https://doi.org/10.1016/j.ijrefrig.2004.08.016

Patel, A. (2023). *Heat Exchangers in Industrial Applications : Efficiency and Optimization Strategies*. *September*. https://doi.org/10.17577/IJERTV12IS090003

ACKNOWLEDGEMENT

We would like to express our gratitude to Friterm, the company we work for, for their permission to use the products and measurement tools in this study, as well as for their support towards academic research. Additionally, we extend our thanks to Professor Dr. Feridun Ozguc for his assistance in this study.